Towards robust optimal control of chromatographic separation processes with controlled flow reversal

Dominik H. Cebulla[1,*], **Christian Kirches**[1,**], and **Andreas Potschka**[3,***]

[1] TU Braunschweig, Institute for Mathematical Optimization, Universitätsplatz 2, D-38106 Braunschweig
[3] Clausthal University of Technology, Institute of Mathematics, Erzstraße 1, D-38678 Clausthal–Zellerfeld

Column liquid chromatography is an important technique applied in the production of biopharmaceuticals, specifically for the separation of biological macromolecules such as proteins. When setting up process conditions, it is crucial that the purity of the product is sufficiently high, even in the presence of perturbations in the process conditions, e.g., altered buffer salt concentrations. Our goal is to employ a model-based approach for robust process optimization where we aim to safeguard the purity level of the product against uncertainties in the model parameters. Furthermore, we include the possibility of reversing the flow direction as an additional time-dependent control degree of freedom, as a flow reversal is often performed in practice to achieve better separation.

We present a strategy where a flow reversal is incorporated effectively in a mathematical model for column chromatography, eventually leading to the challenging class of mixed-integer optimal control problems constrained by advection-diffusion-reaction-type partial differential equations. Furthermore, we examine a sampling-based strategy towards robustly optimal switching control applied to chromatographic separation processes. By means of a computational study, we discuss the quality of the presented approach and how reversing the flow direction may play a role in terms of the quality of the solutions.

1 Introduction

Column chromatography is the method of choice in the so-called downstream processing of biopharmaceuticals, where the goal is to extract and purify certain proteins from a mixture containing impurities such as host cell proteins and viruses [1]. Since the costs of chromatography steps constitute a significant amount of the total costs in the downstream processing, it is natural to consider optimization of chromatographic separation processes, e.g., by means of a model-based approach.

However, due to the complex nature of chromatographic processes, there are various sources of uncertainties involved, e.g., plant-model mismatches and uncertain model parameters, but also perturbations in the applied controls in real-world applications. It is thus important to safeguard against these types of uncertainties, as the purity of the product must remain within specifications.

As an additional aspect, we note that the flow direction can often be reversed in real-world chromatographic applications, typically leading to sharper elution profiles. It should hence be advantageous to incorporate such a flow reversal as an additional process control that can be optimized.

Related work: Since robustness is such an important aspect in chromatographic separation processes, this problem has already received considerable interest. One particular strategy to achieve a robust separation is by determination of so-called pooling strategies, i.e., to determine when the eluate should be collected or not. Usually, a nominal point of operation is set up and the process controls and/or model parameters are then slightly perturbed to investigate how these perturbations affect purity and yield of the product, see, e.g., [2,3]. A different approach is by application of closed-loop optimal control, such as model predictive control [4,5] or set point optimization strategies [6], where the control scheme is adapted online to counteract measured deviations in the state space.

To the best of our knowledge, there are no approaches to regard a flow reversal as a free process control in batch-operated chromatographic processes. The modeling platform CADET [7] provides the possibility to model complex networks of connections between chromatography columns, tubings, continuous stirred tanks, etc. Hence, a flow reversal can be simulated by using different flow paths, called "valve switches" in CADET, but the configurations themselves cannot be optimized, but are chosen beforehand and fixed. A loosely related task is described in [8], where an optimal plant configuration is determined with a hierarchical approach. Here, the ordering of several columns, which can vary over time, is to be optimized. Lastly, optimization of a simulated moving bed (SMB) chromatography process, where optimal valve switches are determined by setting up a mixed-integer optimal control problem (MIOCP), is described in [9]. Although the SMB process mimics a countercurrent flow between mobile and stationary phase, no actual flow reversal is performed.

* Corresponding author: e-mail d.cebulla@tu-bs.de, orcid 0000-0002-3025-8673
** e-mail c.kirches@tu-bs.de, orcid 0000-0002-3441-8822
*** e-mail andreas.potschka@tu-clausthal.de, orcid 0000-0002-6027-616X

Contributions: First, we propose a modeling approach for flow reversal in a column chromatography process, where, e.g., the spatial discretization scheme for the underlying partial differential equation (PDE) model does not have to be adapted. Second, we investigate a sampling-based approach for robust optimization of chromatographic separation processes and discuss whether a flow reversal can be beneficial for a robust process strategy.

2 A mathematical model for column chromatography with flow reversal

In column liquid chromatography, a liquid solvent (mobile phase) is pumped through a column that is typically packed with porous particles (particle/stationary phase). Separation of a mixture is achieved by exploiting the substances' different retention times, the latter being affected, e.g., by the interaction of a substance with the stationary phase. In this section, we first outline the equilibrium-dispersive model that describes the column chromatography process, followed by a brief discussion of two possible flow reversal implementations.

2.1 Equilibrium-dispersive model for column chromatography

We consider an equilibrium-dispersive model (EDM), see [10, section 6.2.4.1] to describe the following phenomena occurring in column chromatography processes: transport of the substances within the column, axial dispersion, and adsorption processes. We employ a multi-component Langmuir isotherm model with mobile phase modulator to describe the adsorption process, see [11,12]. This adsorption model can be used to describe various chromatography techniques, such as ion exchange chromatography, hydrophobic interaction chromatography, and reversed-phase chromatography.

The EDM in combination with the Langmuir isotherm model describes the concentration profiles of all components i along the axial position $x \in (0, L_c)$ of the column for a given time $t \in (0, t_f)$,

$$\frac{\partial c_{m,i}}{\partial t}(t,x) = -\frac{v_{\mathrm{sup}}}{\varepsilon_t}\frac{\partial c_{m,i}}{\partial x}(t,x) + \widetilde{D}_{\mathrm{app},i}\frac{\partial^2 c_{m,i}}{\partial x^2}(t,x) - \frac{1-\varepsilon_t}{\varepsilon_t}\frac{\partial q_i}{\partial t}(t,x), \tag{1a}$$

$$\frac{\partial q_i}{\partial t}(t,x) = k_{\mathrm{kin},i}\left[K_{0,i}\, q_{\mathrm{max},i}\, e^{\gamma_{\mathrm{salt},i}\, c_{m,\mathrm{salt}}(t,x)}\, c_{m,i}(t,x)\left(1 - \sum_{j=1}^{n_{\mathrm{comp}}} \frac{q_j(t,x)}{q_{\mathrm{max},j}}\right) - q_i(t,x)\right], \tag{1b}$$

$$\frac{\partial q_{\mathrm{salt}}}{\partial t}(t,x) = 0. \tag{1c}$$

The states in the EDM (1) are the concentrations in the mobile phase $c_{m,i}$ and the adsorbed phase q_i, respectively. We remark that (1a) holds for all components $i \in \{1,\dots,n_{\mathrm{comp}}\} \cup \{\mathrm{salt}\}$, whereas (1b) holds for $i \in \{1,\dots,n_{\mathrm{comp}}\}$. The mobile phase modulator component is here denoted by "salt".

Model parameters occurring in (1) are the total porosity ε_t, the modified apparent dispersion coefficient $\widetilde{D}_{\mathrm{app}}$, as well as adsorption-related parameters k_{kin}, K_0, γ_{salt}, and q_{max}. Lastly, v_{sup} is the superficial flow velocity, which is typically computed from a prescribed volumetric flow rate $\dot{V}$.

The boundary conditions for the PDE model (1) are

$$\frac{\partial c_{m,i}}{\partial x}(t,0) = \frac{v_{\mathrm{sup}}}{\varepsilon_t \widetilde{D}_{\mathrm{app},i}}\left(c_{m,i}(t,0) - c_{\mathrm{in},i}(t)\right), \quad \frac{\partial c_{m,i}}{\partial x}(t,L_c) = 0, \tag{2}$$

for $i \in \{1,\dots,n_{\mathrm{comp}}\} \cup \{\mathrm{salt}\}$ and $t \in [0,t_f]$. Here, $c_{\mathrm{in},i}(\,\cdot\,)$ is the inlet concentration of component i, a time-dependent control degree of freedom. Furthermore, the initial conditions read for $x \in [0,L_c]$ and $i \in \{1,\dots,n_{\mathrm{comp}}\}$

$$c_{m,i}(0,x) = 0, \quad q_i(0,x) = 0, \quad c_{m,\mathrm{salt}}(0,x) = c_{\mathrm{salt,init}}, \quad q_{\mathrm{salt}}(0,x) = 0, \tag{3}$$

which corresponds to an equilibrated column. This means that no mixture is present in the column and an initial salt concentration $c_{\mathrm{salt,init}}$, which is a time- and space-independent control degree of freedom, is chosen.

2.2 Flow reversal

Our goal is to compute an optimal control strategy where it is decided whether one or more flow reversals should be performed or not. Therefore it is natural to introduce a binary-valued control function, here denoted by $\mathrm{flip}(\,\cdot\,)$, which signifies whether the flow is reversed or not. In the following, we discuss two approaches to incorporate a change in the flow direction, which are also visualized in figure 1.

The first idea, shown in the left picture of figure 1, is based on the idea that reversing the flow direction corresponds to flipping the sign of the flow velocity v_{sup} in (1). This could be achieved, e.g., by replacing v_{sup} with $(1 - 2 \cdot \mathrm{flip}(t))v_{\mathrm{sup}}$ in (1a). Although this strategy seems very natural, it has certain drawbacks. For example, if the flow is reversed, then the numerical discretization scheme for the spatial discretization of the PDE model must be adapted for the sake of numerical stability. Furthermore, since also the roles of inflow and outflow change, the boundary conditions must be adapted as well.

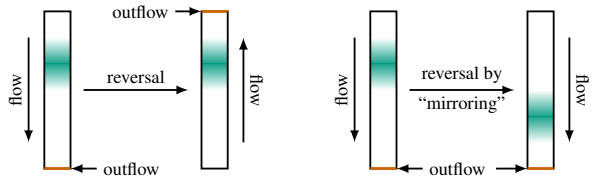

Fig. 1: Two possible approaches to incorporate a flow reversal in a column chromatography model. Left: The flow direction is reversed, e.g., by flipping the sign of the flow velocity v_{sup} in (1). Consequently, the roles of outflow and inflow change. Right: The flow direction is reversed by "flipping" the column, i.e., by mirroring the concentration profiles, but keeping the flow direction. Here, the roles of outflow and inflow do not change.

A different strategy to implement a flow reversal, shown in the right picture of figure 1, is by "flipping" the column, i.e., mirroring the concentration profiles, while keeping the flow direction. Then, the outflow remains at $x = L_c$ and also the spatial discretization scheme for the numerical solution of the PDE does not have to be adapted. We note, however, that this strategy is more apt to be implemented directly on a fully discretized problem. Since we later employ a direct "first discretize, then optimize" approach to solve the MIOCPs introduced in section 3.1, this is not a major drawback and hence we use this second approach later in our case study. Note that a mathematical formulation for implementing the second strategy on the nonlinear program (NLP) level is given in (8) in section 3.2.

3 Optimization of column chromatography processes

In this section, we first introduce a possible optimal control problem formulation for chromatographic separation processes, followed by a brief presentation of the numerical solution approach. For the latter, we specifically emphasize how the flow reversal is implemented in practice.

3.1 A mixed-integer optimal control problem for column chromatography

When optimizing chromatography processes, typical quantities of interest are yield and purity of the product(s), batch-cycle times, and productivity of the separation process, see [10, chapter 7]. Here, we focus on yield and purity of the product, and we aim to maximize the yield while ensuring a certain level of purity.

To define yield and purity of a component $i \in \{1, \dots, n_{\text{comp}}\}$, we introduce the injected and collected amounts of substance, which are for $t \in [0, t_f]$ given by

$$m_{\text{in},i}(t) = \dot{V} \int_0^t c_{\text{in},i}(\tau)\, \mathrm{d}\tau, \qquad m_{\text{coll},i}(t) = \dot{V} \int_0^t c_{\text{out},i}(\tau)\, \text{coll}(\tau)\, \mathrm{d}\tau. \tag{4}$$

Here, $\text{coll} \in L^\infty([0, t_f], \{0, 1\})$ is a binary control that signifies whether the eluate is collected or not and $c_{\text{out},i}$ is the concentration of component i leaving the column. Here, $c_{\text{out},i}(t) \coloneqq c_{m,i}(t, L_c)$. Based on these quantities, yield and purity of a component i are defined by

$$\text{Yield}_i(t) = \frac{m_{\text{coll},i}(t)}{m_{\text{in},i}(t)}, \qquad \text{Purity}_i(t) = \frac{m_{\text{coll},i}(t)}{\sum_{j=1}^{n_{\text{comp}}} m_{\text{coll},j}(t)}.$$

We can now define the MIOCP that we are considering in our case study in section 5. Using a rather high-level problem formulation, we solve

$$\begin{aligned} \inf_{\substack{\text{coll}(\cdot),\, c_{\text{in,salt}}(\cdot),\\ c_{\text{salt,init}},\text{flip}(\,\cdot\,)}} \quad & -\text{Yield}_\star(t_f) + \text{control regularization terms (6)} \\ \text{s.t.} \quad & \text{Purity}_\star(t_f) \geq \text{Purity}_{\min,\star}, \\ & + \text{PDE constraints (1)–(3) and ODE constraints (4)}, \\ & + \text{further control constraints (7)}. \end{aligned} \tag{5}$$

The goal of this formulation is to maximize the yield of a product component, denoted by $\star$, while also achieving a certain purity level. We remark that the binary control function $\text{flip} \in L^\infty([0, t_f], \{0, 1\})$ is used to model the flow reversal and has been informally introduced in section 2.2. The specific implementation is shown in (8) in section 3.2.

Before we explain the control regularization terms and constraints in more detail, we point out that it is also possible to extend this formulation when one is interested in more than one product component. In this case, one could replace yield and purity by sums of yields and purities of the respective components of interest.

As control regularization terms we use L^1 norms for the binary controls and L^2 norms for continuous controls. More precisely, the control regularization terms are chosen as

$$\begin{aligned}&\text{control regularization terms } =\\ &\xi_{\text{coll}} \int_0^{t_f} |\text{coll}(t) - \text{coll}_{\text{ref}}| \,\mathrm{d}t + \xi_{\text{flip}} \int_0^{t_f} |\text{flip}(t) - \text{flip}_{\text{ref}}| \,\mathrm{d}t + \xi_{c_{\text{in,salt}}} \int_0^{t_f} (c_{\text{in,salt}}(t) - c_{\text{in,salt,ref}})^2 \,\mathrm{d}t, \end{aligned} \tag{6}$$

where the $\xi_\circ$ are suitable weights and $\circ_{\text{ref}}$ are the regularization values for $\circ \in \{\text{coll}, \text{flip}, c_{\text{in,salt}}\}$.

In our case study, we add further control constraints to (5) to reflect an experiment with two phases. In the first phase, the mixture is injected into the system for a prescribed amount of time $t_{\text{inj}} \in (0, t_f)$ and with given sample concentrations $c_{\text{load},i}$, the latter being additional model parameters. During this time period, the buffer composition cannot be changed, typically, and hence we require the salt inlet $c_{\text{in,salt}}(\,\cdot\,)$ to remain fixed during this phase. Furthermore, the flow direction is not reversed in this phase. In the second phase, the sample injection is stopped and the salt inlet and flow reversal is free for optimization to eventually elute the product.

Mathematically, we obtain the following constraints for a.a. $t \in [0, t_f]$

$$\begin{aligned}&\text{control constraints:}\\ &c_{\text{in},i}(t) &&= \begin{cases} c_{\text{load},i}, & \text{if } 0 \le t \le t_{\text{inj}},\\ 0, & \text{if } t > t_{\text{inj}}, \end{cases} && \text{for } i \in \{1, \dots, n_{\text{comp}}\},\\ &c_{\text{in,salt}}(t) &&\in \left[\underline{c_{\text{in,salt}}}, \overline{c_{\text{in,salt}}}\right], &&\\ &c_{\text{in,salt}}(t) &&= c_{\text{salt,init}}, && \text{for a.a. } 0 \le t \le t_{\text{inj}},\\ &\text{flip}(t) &&= 0, && \text{for a.a. } 0 \le t \le t_{\text{inj}},\\ &\text{coll}(t) &&\in \{0, 1\}, &&\\ &\text{flip}(t) &&\in \{0, 1\}. && \end{aligned} \tag{7}$$

Here, $\underline{c_{\text{in,salt}}}$ is a lower bound and $\overline{c_{\text{in,salt}}}$ is an upper bound on the salt inlet concentration. Furthermore, the constraint on $\text{flip}(\,\cdot\,)$ during sample injection ensures that no flow reversal can be performed in this phase.

3.2 Numerical solution strategy

To solve (5) we purse a direct "first discretize, then optimize" approach. A detailed description in the context of chromatographic processes is described in [13] and we therefore only state the main steps. Most importantly, we present how the flow reversal is realized in the discretized problem formulation.

First, the PDE model (1) is spatially semi-discretized, see section 5.1 for more details, thus replacing all PDEs by systems of ODEs. Subsequently, we transform the resulting ODE-constrained MIOCP into a continuous optimal control problem by relaxing the binary controls $\text{coll}(\,\cdot\,)$ and $\text{flip}(\,\cdot\,)$ to $[0, 1]$. We highlight that if we consider the control $\text{flip}(\,\cdot\,)$ as fixed and binary-valued, then simply relaxing the only remaining binary control $\text{coll}(\,\cdot\,)$ yields a so-called partially outer convexified and relaxed form, see [14]. We will see that this argument does not work if $\text{flip}(\,\cdot\,)$ is not binary-valued, as this control does not enter the right-hand side of the differential equation system, but it modifies the initial values, see (8).

Afterwards, we transform the continuous optimal control problem into an NLP by using the direct single shooting approach, see [15]. To this end, we partition the time horizon into a control grid $0 = t_0 < \dots < t_{N_{\text{C}}} = t_f$ with $N_{\text{C}} \in \mathbb{N}$ control intervals and we choose all controls to be piecewise constant. Furthermore, we assume that the injection time t_{inj} corresponds to exactly one grid point of the control grid, hence the constraints in the injection phase, see (7), can be easily implemented.

After spatial semi-discretization, relaxation, and control discretization, we obtain the following NLP:

$$\min_{\substack{\text{coll},\, c_{\text{in,salt}},\\ c_{\text{salt,init}},\, \text{flip}}} \quad -\text{Yield}_\star(t_f) + \text{control regularization terms (6)} \tag{8a}$$

$$\begin{aligned}
\text{s.t.}\quad & \text{Purity}_\star(t_f) && \ge \text{Purity}_{\star,\text{min}}, && && (8b)\\
& y^-(0) && = y_0(c_{\text{salt,init}}), && && (8c)\\
\text{For } & 0 \le k < N_{\text{C}}: && && && \\
& y^+(t_k) && = (1 - \text{flip}_k)\, y^-(t_k) + \text{flip}_k\, \mathcal{F}\, y^-(t_k) && && (8d)\\
& \dot{y}(t) && = f(y(t), \text{coll}_k,\, c_{\text{in,salt},k}), && t \in (t_k, t_{k+1}), && (8e)\\
& y^-(t_{k+1}) && = (1 - \text{flip}_k)\, y(t_{k+1}) + \text{flip}_k\, \mathcal{F}\, y(t_{k+1}) && && (8f)\\
& \text{coll}_k && \in [0, 1], \quad \text{flip}_k \in [0, 1], \quad c_{\text{in,salt},k} \in [\underline{c_{\text{in,salt}}}, \overline{c_{\text{in,salt}}}] && && (8g)\\
& && + \text{constraints in injection phase, see (7).} && && (8h)
\end{aligned}$$

We briefly discuss the important parts of the above problem formulation: All controls are now vectors with N_C entries, with, e.g., $\mathrm{coll}(t) = \mathrm{coll}_k$ for $t \in (t_k, t_{k+1})$ and $0 \leq k < N_\mathrm{C}$ (analogously for the other controls). The quantity y contains the states from the spatially semi-discretized PDE and additional ODE states stemming from, e.g., the amounts of substances and the control regularization terms, see (4) and (6). Furthermore, f denotes the corresponding right-hand side.

The flow reversal is implemented in (8d)–(8f) as follows: Given an initial value $y^-(t_k)$, if $\mathrm{flip}_k = 1$, we modify the states to mirror the concentration profiles via (8d). If $\mathrm{flip}_k = 0$, the states are not modified. Here, $\mathcal{F}$ is a matrix which mirrors the concentration profiles of the spatially semi-discretized PDE model (1). If y would only contain the semi-discretized PDE states, then mirroring is achieved by choosing $\mathcal{F}$ as the flipped identity matrix, i.e., where the ones are contained on the counter diagonal. Then, the initial value problem is solved, see (8e), and the concentration profiles are mirrored again, if necessary, in (8f). Here, $y(t_{k+1})$ denotes the solution of the initial value problem (8d)–(8e).

Of course, this transformation only makes sense if $\mathrm{flip}_k \in \{0, 1\}$. Hence we state the following assumption:

Assumption 3.1 We assume that there exists $N_\mathrm{C} \in \mathbb{N}$ and a control grid $0 = t_0 < \cdots < t_{N_\mathrm{C}} = t_f$ such that a solution of (8) satisfies $\mathrm{flip}_k \in \{0, 1\}$ for all $0 \leq k < N_\mathrm{C}$.

We agree that this assumption may seem rather strict, but in most case studies (the ones shown in section 5, as well as others) we could observe that flip_k was always very close to being binary-valued for all $0 \leq k < N_\mathrm{C}$. To back up such a bang-bang behavior theoretically one could potentially use a variant of Pontryagin's maximum principle for switched dynamical systems, see, e.g., [16]. However, due to the complex problem we are considering this is by no means trivial.

Note that we do not make any assumptions regarding the feasibility of the eluate collection control $\mathrm{coll}(\,\cdot\,)$ for the MIOCP (5). Although we observe that this control is also already binary-valued in our case studies, we can also apply the so-called sum-up rounding procedure [14], which has provable approximation properties leading to δ-feasible and δ-optimal controls, see [17]. We highlight that this argument only works if the flip control is already discrete feasible, before any further rounding is applied. If the flip control is not feasible, then the initial values, see (8d), are perturbed and the error in the states cannot be arbitrarily diminished.

4 A sampling-based robust optimization strategy

In this section, we briefly describe a sampling-based strategy that we apply for the robust optimization of chromatographic processes, focusing on robustification with respect to uncertain model parameters occurring in (1). To focus on the key aspects, we discuss the robustification strategies based on the following formulation, compare (5):

$$\begin{aligned} \inf_{\substack{\mathrm{coll}(\cdot),\, c_{\mathrm{in,salt}}(\cdot),\\ c_{\mathrm{salt,init}},\, \mathrm{flip}(\cdot)}} \quad & -\mathrm{Yield}_\star(t_f, p) + \text{control regularization terms (6)} \\ \text{s.t.} \quad & \mathrm{Purity}_\star(t_f, p) \geq \mathrm{Purity}_{\star,\mathrm{min}}, \\ & + \text{PDE constraints (1)–(3) and ODE constraints (4)}, \\ & + \text{further control constraints (7)}. \end{aligned}$$

In contrast to (5), we explicitly highlight the parameter-dependency of yield and purity in this formulation. Furthermore, in the following presentation $\bar{p} \in \mathbb{R}^{n_p}$ denotes the *nominal* parameter and the corresponding MIOCP with the choice $p = \bar{p}$ is accordingly called the *nominal* optimal control problem.

Let $\mathcal{P} \subseteq \mathbb{R}^{n_p}$ with $\bar{p} \in \mathcal{P}$. We call $\mathcal{P}$ an uncertainty set; it can correspond to, e.g., confidence or credible regions that have been determined in the parameter estimation context. Our goal is to robustify the chromatographic process against all possible parameters from the uncertainty set. We thus solve

$$\begin{aligned} \inf_{\substack{s, \mathrm{coll}(\cdot),\, c_{\mathrm{in,salt}}(\cdot),\\ c_{\mathrm{salt,init}},\, \mathrm{flip}(\cdot)}} \quad & -s + \text{control regularization terms (6)} \\ \text{s.t.} \quad & \mathrm{Yield}_\star(t_f, p) \geq s, && \text{for all } p \in \mathcal{P}, \\ & \mathrm{Purity}_\star(t_f, p) \geq \mathrm{Purity}_{\star,\mathrm{min}}, && \text{for all } p \in \mathcal{P}, \\ & + \text{PDE constraints (1)–(3) and ODE constraints (4)}, \\ & + \text{further control constraints (7)}. \end{aligned} \tag{9}$$

Here, $s \in \mathbb{R}$ is a newly introduced slack variable that serves as a bound for all obtained yields. When considering a single product component, we have $s \in [0, 1]$ in the optimum (if it exists).

Typically, $\mathcal{P}$ contains infinitely many elements and, correspondingly, (9) has infinitely many constraints. To cope with this situation, a straightforward idea is to require that the yield and purity constraints must only be fulfilled for certain *sample*

parameters $p^{(1)}, \dots, p^{(N)} \in \mathcal{P}$. We thus instead solve

$$\begin{aligned} \inf_{\substack{s,\mathrm{coll}(\cdot),\, c_{\mathrm{in,salt}}(\cdot),\\ c_{\mathrm{salt,init}},\, \mathrm{flip}(\cdot)}} \quad & -s + \text{control regularization terms (6)} \\ \text{s.t.} \quad & \mathrm{Yield}_\star(t_f, p) \geq s, && \text{for all } p \in \{p^{(1)}, \dots, p^{(N)}\} \subseteq \mathcal{P}, \\ & \mathrm{Purity}_\star(t_f, p) \geq \mathrm{Purity}_{\star,\mathrm{min}}, && \text{for all } p \in \{p^{(1)}, \dots, p^{(N)}\} \subseteq \mathcal{P}, \\ & + \text{ PDE constraints (1)–(3) and ODE constraints (4),} \\ & + \text{ further control constraints (7).} \end{aligned} \tag{10}$$

Unfortunately, it is not clear which and how many parameter samples to take. It is shown in [18] for convex optimization problems that the probability of constraint violation can be controlled by the number of chosen samples. Although this result is not applicable in our case, we are motivated to pursue this strategy.

Yet, solving (9) for finitely, but possibly many parameter samples is still prohibitively expensive. We hence propose to pursue the following approach: We perform simulations of the chromatography process for many parameter samples, as this is much cheaper than solving MIOCPs with many constraints. Then, we take a small selection of the "worst" parameter samples and solve (9) with those. Of course, it is not clear what the worst parameter samples are; in our case study in section 5 we take the set of parameters that contains the nominal parameter $\bar{p}$, the three parameters that lead to the worst yield and purity, respectively, as well as the parameters that correspond to the leftmost and rightmost peaks of the product component.

5 Computational results

We now present a case study for robust optimization of chromatographic separation processes. We first outline the general setting, followed by the actual presentation and discussion of the obtained results.

5.1 Setting

In our case study we examine a separation process where one product component is to be separated from two impurity components; the purity requirement is set to $\mathrm{Purity}_{\star,\mathrm{min}} = 0.95$. The model parameters are summarized in table 1 and are chosen such that they reflect plausible values. For the control regularization, see (6), we choose $\xi_{\mathrm{coll}} = \xi_{\mathrm{flip}} = 5 \cdot 10^{-3}$ and $\xi_{c_{\mathrm{in,salt}}} = 10^{-2}$, as well as $\mathrm{coll}_{\mathrm{ref}} = 0$, $\mathrm{flip}_{\mathrm{ref}} = 1$, and $c_{\mathrm{in,salt,ref}} = 0.1\,\mathrm{M}$.

We set $t_f = 5\,\mathrm{min}$ and the control grid is discretized using $N_{\mathrm{C}} = 60$ equidistant intervals. Each cell has thus a length of $\Delta t = 5\,\mathrm{s}$. The sample injection time is $t_{\mathrm{inj}} = 10\,\mathrm{s}$. The PDE model (1) is spatially semi-discretized with a higher-order finite volume scheme using 75 equidistant cells. More precisely, we use a WENO35 scheme and replace the nonlinear weights by the respective linear ones. We already applied and summarized this scheme elsewhere [13] and refer to this source for further details.

The computational experiments are performed on an Ubuntu 24.04 system powered by an Intel Core i7-10700 with 64 GB of main memory. All variants of optimal control problems are prototypically implemented in MATLAB using CasADi 3.7.0 [19]. We use CasADi's interface to IDAS as an integrator and `IPOPT` as NLP solver. For the integrator IDAS we set the maximum order to four. For `IPOPT`, we use a limited-memory BFGS approximation for the Hessian and we set the option `acceptable_tol` to 10^{-3} and `acceptable_iter` to 5. The motivation for this choice is to speed up the computations, as we made the observation that the dual infeasibility cannot be reduced to an arbitrary small value, although primal feasibility and complementarity is well achieved and the objective function value does not change anymore in later iterations.

To assess the robustness of the separation process we define our uncertainty set as follows: All model parameters occurring in (1), as well as the sample injection concentration c_{load} are perturbed to obtain new parameter samples. More precisely, when $\bar{p}_i$ denotes the ith nominal parameter, see table 1, then a new parameter sample is drawn according to $p_i := (1 + \varepsilon_i)\bar{p}_i$, where $\varepsilon_i \sim \mathcal{N}(0, 0.02^2)$, i.e., each parameter is perturbed by a normally distributed error with 2% relative standard deviation.

Table 1: Model parameters and further quantities used in the equilibrium-dispersive model (1) for the case study.

Quantity	Value	Unit	Quantity	Value	Unit
v_{sup}	5.09×10^{0}	$\mathrm{cm\,min^{-1}}$	$K_{0,1}$	1.00×10^{2}	$\mathrm{M^{-1}}$
L_c	2.50×10^{0}	cm	$K_{0,2}$	1.50×10^{2}	$\mathrm{M^{-1}}$
$c_{\mathrm{load},\{1,2,3\}}$	1.00×10^{-4}	M	$K_{0,3}$	2.00×10^{2}	$\mathrm{M^{-1}}$
$\widetilde{D}_{\mathrm{app},\{1,2,3\}}$	1.00×10^{-2}	$\mathrm{cm^2\,min^{-1}}$	$q_{\mathrm{max},\{1,2,3\}}$	3.50×10^{-1}	M
$\widetilde{D}_{\mathrm{app,salt}}$	1.00×10^{-1}	$\mathrm{cm^2\,min^{-1}}$	$\gamma_{\mathrm{salt},1}$	-5.00×10^{0}	$\mathrm{M^{-1}}$
ε_t	8.00×10^{-1}	—	$\gamma_{\mathrm{salt},2}$	-4.00×10^{0}	$\mathrm{M^{-1}}$
$k_{\mathrm{kin},\{1,2,3\}}$	5.00×10^{2}	$\mathrm{min^{-1}}$	$\gamma_{\mathrm{salt},3}$	-3.00×10^{0}	$\mathrm{M^{-1}}$

We compute eleven uncertainty sets $\mathcal{P}^{(0)}, \dots, \mathcal{P}^{(10)}$, each containing 200 randomly drawn samples. The reference uncertainty set used for optimization is $\mathcal{P}^{(0)}$.

5.2 Results and discussion

We depict in figure 2 the concentration profiles when using our initial (control) guess. The actual profiles, i.e., using the nominal parameters, are drawn with colored lines with an additional inner solid black line. The other profiles, stemming from using the perturbed parameters $p \in \mathcal{P}^{(0)}$, are drawn with the same color, but higher transparency.

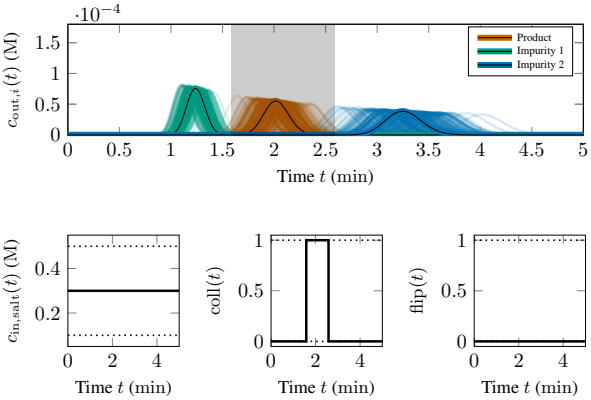

Fig. 2: Nominal concentration profiles (colored lines with inner black line) when applying the initially chosen controls, as well as concentration profiles obtained by using parameters from $\mathcal{P}^{(0)}$. The gray-shaded area depicts where the eluate is collected. Although an almost perfect separation is achieved for the nominal parameters, using perturbed parameters leads to overlapping peaks.

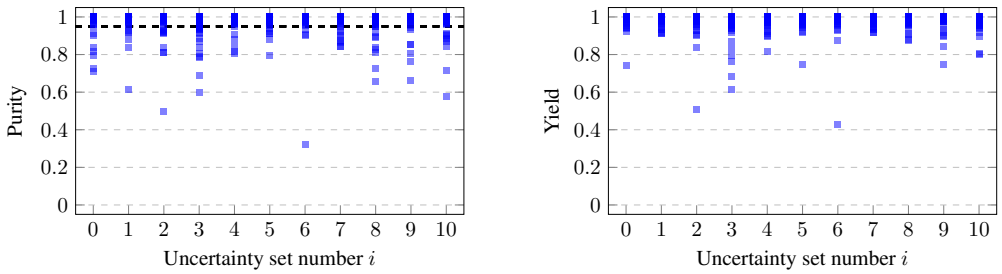

Fig. 3: Obtained purities (left) and yields (right) when applying the controls shown in figure 2 and using the parameter samples from $\mathcal{P}^{(i)}$, $i \in \{0, \dots, 10\}$. The purity requirement of 95% is violated between four and seventeen times.

Although the initial guess already achieves a good separation with yield and purity of more than 99.9%, the results deteriorate when we investigate the sampled concentration profiles using the uncertainty set $\mathcal{P}^{(0)}$ (top picture). There, we observe that a significant overlap of peaks is present, leading to worse yields and purities, also see figure 3. In fact, the purity requirement is violated between 4 and 17 times. Setting the yield to zero whenever the purity requirement is violated, we note that the average yield ranges from 91% to 97.6% for all uncertainty sets $\mathcal{P}^{(i)}$, whereas the average purity ranges from 98.6% to 99.4%. Hence the mean purity is always much higher than the demanded 95%, but the average yield varies quite strongly.

Solving the nominal MIOCPs (5), once with free and once with fixed flow reversal control, leads to the optimized concentration profiles and controls shown in figure 4. In the case where the flow reversal is a free control, the second impurity "vanishes", i.e., it remains inside the column for the whole process duration. When no flow reversal is performed, the second impurity elutes very slowly due to the low salt concentration. Moreover, when using perturbed parameters from the uncertainty set $\mathcal{P}^{(0)}$, the second impurity peaks shift significantly.

When the flow reversal is a degree of freedom, the purity requirement is violated between zero and two times and the average purity ranges from 99.65% to 99.85% and the average yield ranges from 97.85% to 99.6% for all uncertainty sets $\mathcal{P}^{(i)}$ (again, setting the yield to zero whenever the purity constraint is violated). On the other hand, when the flow direction cannot be changed, the purity requirement is violated between zero and eight times and the average purity ranges from 99.45% to 99.8% and the average yield ranges from 95.4% to 99.5%. Hence, in the nominal case we observe that performing a flow reversal leads to slightly better results, particularly in terms of the obtained yield. Furthermore, we note a considerable improvement compared to the non-optimized case depicted in figure 2.

Lastly, we investigate the sampling-based robustification strategy presented in section 4. As described earlier, we take the set $\mathcal{P}^{(0)}$ as reference set and choose the nominal parameter $\bar{p}$, the parameter samples corresponding to the three worst yields

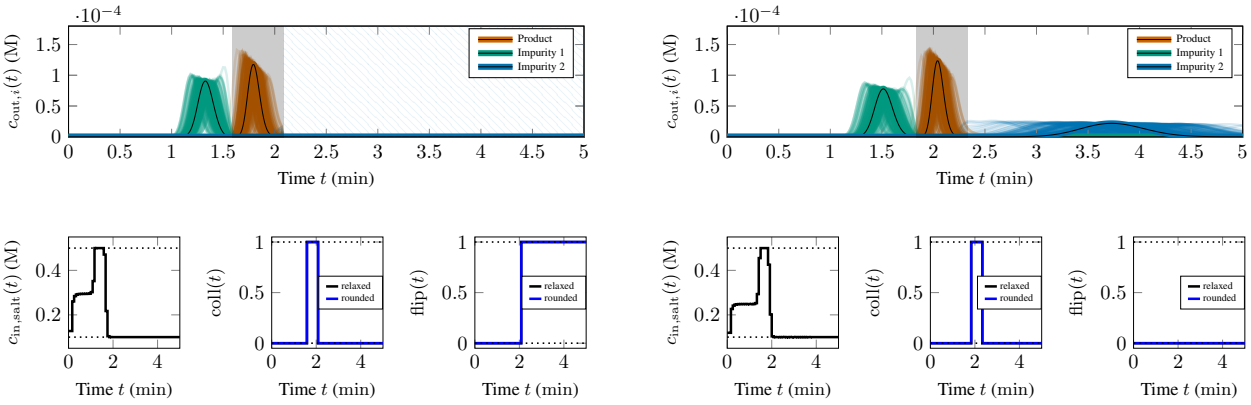

Fig. 4: Nominal concentration profiles (colored lines with inner black line) when applying the optimized controls from solving the nominal MIOCP (5), as well as concentration profiles obtained by using parameters from $\mathcal{P}^{(0)}$. The gray-shaded area depicts where the eluate is collected, the blue crosshatched area shows where the flow is reversed. Left: The flow reversal is a free control. Right: No flow reversal is possible.

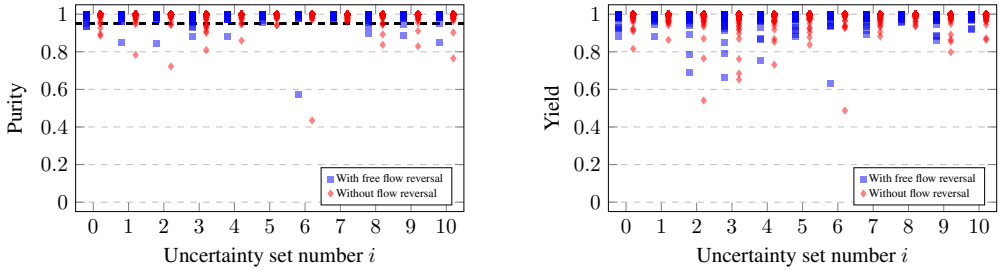

Fig. 5: Obtained purities (left) and yields (right) when applying the controls shown in figure 4 and using the parameter samples from $\mathcal{P}^{(i)}$, $i \in \{0, \dots, 10\}$. With a free flow reversal control, we observe that the purity requirement of 95% is violated between zero and two times. Without performing a flow reversal, the purity requirement of 95% is violated between zero and eight times.

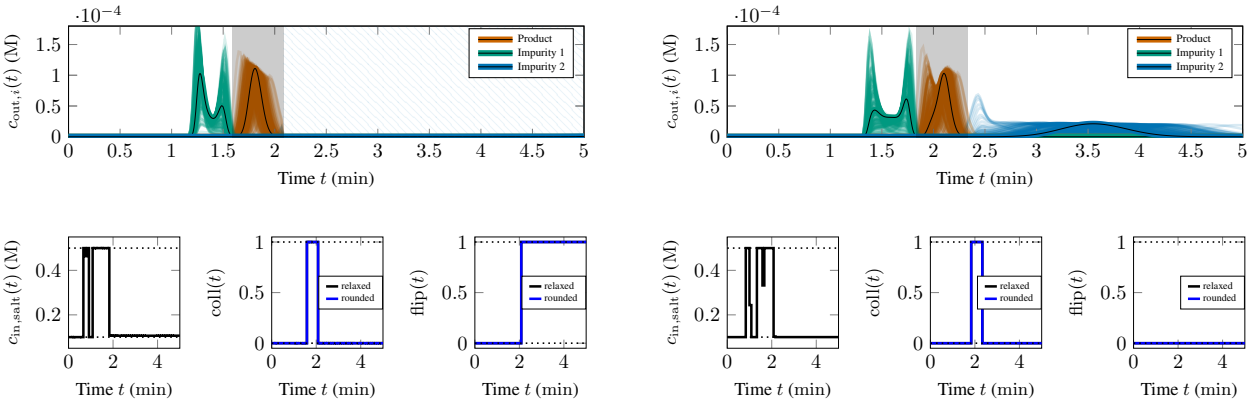

Fig. 6: Nominal concentration profiles (colored lines with inner black line) when applying the optimized controls from solving the robustified MIOCP (10), as well as concentration profiles obtained by using parameters from $\mathcal{P}^{(0)}$. The gray-shaded area depicts where the eluate is collected, the blue crosshatched area signifies where the flow is reversed. Left: The flow reversal is a free control. Right: No flow reversal is possible. The salt inlet concentration shows in both cases a more varying behavior compared to the nominal case.

and purities, as well as the samples corresponding to the leftmost and rightmost product peaks to solve (10). Furthermore, we use the controls obtained from the respective nominal MIOCP, see figure 4, as initial guess for the controls.

The concentration profiles are shown in figure 6 and the obtained purities and yields are depicted in figure 7. For both variants the purity constraints are very rarely violated, ranging from zero to a maximum of three times (with free flow reversal control) or four times (no flow reversal performed). The purity is hence violated in less that 2% of all cases. As in the nominal case, the yields are typically lower when no flow reversal is performed, but the purities are quite similar, see figure 7. Specifically, when a flow reversal can be applied, the mean of purities ranges from 99.45% to approximately 99.6% and the mean of yields ranges from 97.7% to 99.8% for all uncertainty sets. If no flow reversal is performed, the mean of purities ranges from 99.4% to 99.65% and the mean of yields ranges from 97.4% to 99.6% for all uncertainty sets. We hence note

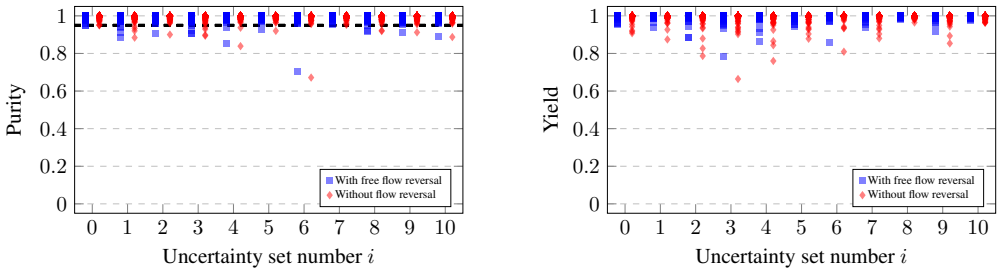

Fig. 7: Obtained purities (left) and yields (right) when applying the controls shown in figure 6 and using the parameter samples from $\mathcal{P}^{(i)}$, $i \in \{0, \dots, 10\}$. With a free flow reversal control, we observe that the purity requirement of 95% is violated between zero and three times. Without performing a flow reversal, the purity requirement of 95% is violated between zero and four times.

that on average the obtained yields are slightly better in the robust solutions compared to the nominal solutions. Furthermore, in the robust solutions the worst case yields are much lower when no flow reversal can be performed compared to the setting where the flow reversal is a degree of freedom. Hence, performing a flow reversal can indeed be advantageous.

When compared to the nominal solution, we see that the salt inlet control is much more varying in the robustified solution, hence the concentration profiles show more complex-shaped peaks than before. Furthermore, it is interesting to note that despite the significantly different salt inlet profiles, the purity requirements are still fulfilled in most cases. Of course, there is no guarantee that this will always be the case and hence more parameter samples must be considered when solving (10).

We also note that although the average purities and yields do not differ too much between the respective nominal and robust solutions, we note that the resulting yields and purities do not spread as much in the robust solution. That is, the worst yields and purities are higher (better) in the robust solution, than in the nominal solutions, see figures 5 and 7.

As a further remark, we note that in the solution for all optimization problems the relaxed (originally binary) controls are already binary-valued, hence feasible for the respective MIOCP formulation. Therefore, applying a rounding procedure has no effect. We thus think that assumption 3.1 is indeed not too strict and often fulfilled in practice.

We want to conclude this section with a quick overview of the required number of iterations and the computational times reported by `IPOPT`. Solving the nominal MIOCPs takes 75 iterations and roughly $550\,\mathrm{s}$ with free flow reversal control and 69 iterations and approximately $410\,\mathrm{s}$ when the flow reversal is fixed at zero. Solving the robustified MIOCP (10) takes 57 iterations and roughly $2220\,\mathrm{s}$ with free flow reversal and 52 iterations and approximately $1700\,\mathrm{s}$ with fixed flow reversal. Hence, as expected the computational effort is much higher in the robust setting and the time per iteration increases approximately by a factor of 5.5.

6 Conclusion and outlook

In the previous sections we introduced an approach for incorporating a flow reversal in column chromatography processes as an additional control degree of freedom and we also presented a sampling-based robustification approach to safeguard the purity level against uncertain model parameters.

In our case study we could see that the possibility for changing the flow direction can lead to higher yields. Yet, the proposed robustification approach did not always ensure that the prescribed purity level of the product component is satisfied for each instance of all uncertainty sets. However, the purity requirement was only violated in at most 2% of all cases. It depends on the particular separation process at hand, whether this number of violations is acceptable in a real-world setting from an economic perspective. We remark that taking more parameter samples into account when solving (10) should decrease the number of instances where the purity constraint is violated, but it also leads to more constraints in the optimal control problem formulation.

Based on the presented results, several open questions arise. For example, the uncertainty sets used in our case study arise from perturbing the model parameters with normally distributed errors. However, this is a mere choice and other definitions of uncertainty sets may be more realistic and suitable.

Furthermore, since process controls such as the salt inlet concentration are often also uncertain in the sense that in real-world applications one cannot expect to steer the concentrations to arbitrary precision, it may also be beneficial to robustify the process against perturbations in the controls.

Lastly, the results one obtains when solving the presented optimal control problems depends, e.g., on the chosen control grid and the reference value for control regularization, see (6). It may hence be beneficial to further study the impact of these quantities in the context of robustly optimizing chromatographic separation processes.

Conflicts of interest: The authors declare no conflicts of interest.

Abbreviations: **EDM**: equilibrium-dispersive model; **MIOCP**: mixed-integer optimal control problem; **NLP**: nonlinear program; **ODE**: ordinary differential equation; **PDE**: partial differential equation;

References

[1] B. G. D. Boedeker, Transfus. Med. Rev. **6**(4), 256–260 (1992).
[2] N. Jakobsson, M. Degerman, E. Stenborg, and B. Nilsson, J. Chromatogr. A **1138**(1–2), 109–119 (2007).
[3] N. Borg, K. Westerberg, S. Schnittert, E. von Lieres, and B. Nilsson, IFAC Proceedings Volumes **45**(2), 991–995 (2012), 7th Vienna International Conference on Mathematical Modelling.
[4] C. Grossmann, G. Ströhlein, M. Morari, and M. Morbidelli, J. Process Control **20**(5), 618–629 (2010).
[5] A. Holmqvist, C. Andersson, F. Magnusson, and J. Åkesson, Processes **3**(3), 568–606 (2015).
[6] M. Behrens, P. Khobkhun, A. Potschka, and S. Engell, Optimizing set point control of the MCSGP process, in: 2014 European Control Conference (ECC), (Strasbourg, France, 2014), pp. 1139–1144.
[7] S. Leweke and E. von Lieres, Comput. Chem. Eng. **113**, 274–294 (2018).
[8] D. Gromov, S. Li, and J. Raisch, IFAC Proceedings Volumes **42**(11), 339–344 (2009), 7th IFAC Symposium on Advanced Control of Chemical Processes.
[9] S. Sager, M. Diehl, G. Singh, A. Küpper, and S. Engell, Determining SMB superstructures by mixed-integer optimal control, in: Operations Research Proceedings 2006, edited by K. H. Waldmann and U. M. Stocker (Springer, Berlin, Heidelberg, 2007), pp. 37–42.
[10] H. Schmidt-Traub, M. Schulte, and A. Seidel-Morgenstern (eds.), Preparative Chromatography, second edition (Wiley–VCH, Weinheim, 2012).
[11] W. R. Melander, Z. El Rassi, and C. Horváth, J. Chromatogr. A **469**, 3–27 (1989).
[12] B. Nilsson and N. Andersson, Simulation of process chromatography, in: Preparative Chromatography for Separation of Proteins, (John Wiley & Sons, 2017), chap. 3, pp. 81–110.
[13] H. G. Bock, D. H. Cebulla, C. Kirches, and A. Potschka, Comput. Chem. Eng. **153**, 107435 (2021).
[14] S. Sager, Numerical methods for mixed-integer optimal control problems (Der andere Verlag, Tönning, Lübeck, Marburg, 2005).
[15] J. Stoer and R. Bulirsch, Introduction to Numerical Analysis, No. 12 in Texts in Applied Mathematics (Springer, 2002).
[16] P. Riedinger, C. Iung, and F. Kratz, European Journal of Control **9**(5), 449–458 (2003).
[17] C. Kirches, F. Lenders, and P. Manns, SIAM J. Control Optim. **58**(34), 1371–1402 (2020).
[18] G. Calafiore and M. C. Campi, Math. Progam. Ser. A **102**(1), 25–46 (2005).
[19] J. A. E. Andersson, J. Gillis, G. Horn, J. B. Rawlings, and M. Diehl, Math. Prog. Comp. **11**(1), 1–36 (2019).